For Darcy flow ($A = 0$)

$0 < \lambda < 0.3$	forced convection	(22a)
$0.3 < \lambda < 35$	mixed convection	(22b)
$35 < \lambda$	free convection.	(22c)

Figures 3 and 4 present the ratios of the local and the total surface heat transfer of the cylinder and that of the flat plate (q_{cyl}/q_{fp}, Q_{cyl}/Q_{fp}) for different values of buoyancy, curvature and non-Darcy parameters (λ, ξ, A). Both the local and the total heat transfer ratios (q_{cyl}/q_{fp}, Q_{cyl}/Q_{fp}) increase with ξ for any given λ. For aiding flow ($\lambda > 0$), q_{cyl}/q_{fp} and Q_{cyl}/Q_{fp} decrease as λ ($\lambda > 0$) increases, but they increase as A increases. However, the opposite trend is observed for the case of opposing flow.

CONCLUSIONS

The skin friction and heat transfer parameters are found to increase with increasing buoyancy force for aiding flow and the opposite trend is observed for opposing flow. The results tend to their forced or free convection values when the buoyancy parameter tends to zero or infinity. The results based on the non-Darcy flow model differ considerably from those obtained by using the classical Darcy flow model. Both the heat transfer and skin friction increase with the curvature parameter.

REFERENCES

1. A. Bejan, The basic scales of natural convection heat and mass transfer in fluids and fluid-saturated porous media, *Int. Commun. Heat Mass Transfer* **14**, 107–123 (1987).
2. O. A. Plumb and J. C. Huenfeld, Non-Darcy natural convection from heated surfaces in saturated porous media, *Int. J. Heat Mass Transfer* **24**, 765–768 (1981).
3. A. Bejan and D. Poulikakos, The non-Darcy regime for vertical boundary layer natural convection in a porous medium, *Int. J. Heat Mass Transfer* **27**, 717–722 (1984).
4. M. Kumari, I. Pop and G. Nath, Non-Darcy natural convection from a heated vertical plate in saturated porous media with mass transfer, *Int. Commun. Heat Mass Transfer* **12**, 337–346 (1985).
5. R. Vasantha, I. Pop and G. Nath, Non-Darcy natural convection over a slender vertical frustrum of a cone in a saturated porous medium, *Int. J. Heat Mass Transfer* **29**, 153–156 (1986).
6. M. Kumari, I. Pop and G. Nath, Non-Darcy natural convection on a vertical cylinder in a saturated porous medium, *Wärme- und Stoffübertr.* **20**, 33–37 (1986).
7. D. B. Ingham, The non-Darcy free convection boundary layer on axisymmetric and two-dimensional bodies of arbitrary shape, *Int. J. Heat Mass Transfer* **29**, 1759–1763 (1986).
8. F. C. Lai and F. A. Kulacki, Non-Darcy convection from horizontal impermeable surfaces in saturated porous media, *Int. J. Heat Mass Transfer* **30**, 2189–2192 (1987).
9. A. Mucoglu and T. S. Chen, Analysis of combined forced and free convection across a horizontal cylinder, *Can. J. Chem. Engng* **55**, 265–271 (1977).
10. P. Cheng, Combined free and forced convection flow about inclined surfaces in porous media, *Int. J. Heat Mass Transfer* **20**, 807–814 (1977).
11. H. B. Keller, Numerical methods in boundary layer theory, *Ann. Rev. Fluid Mech.* **10**, 417 (1978).
12. E. M. Sparrow, R. Eichhorn and J. L. Gregg, Combined forced and free convection in a boundary layer, *Physics Fluids* **2**, 319–328 (1959).

Int. J. Heat Mass Transfer. Vol. 32, No. 1, pp. 187–192, 1989
Printed in Great Britain
0017-9310/89 $3.00 + 0.00

On the heat transfer from a cylindrical fin

VIJAY K. GARG†

Department of Mechanical Engineering, The Ohio State University, Columbus, OH 43210, U.S.A.

and

K. VELUSAMY

Indira Gandhi Centre for Atomic Research, Kalpakkam 603102, India

(*Received* 16 *December* 1987 *and in final form* 10 *May* 1988)

1. INTRODUCTION

HEAT TRANSFER from a fin involves two mechanisms, namely conduction within the fin and convection from the fin surface to the surrounding fluid. The boundary condition at the fin–fluid interface is the continuity of heat flux and temperature. Thus the conduction and convection problems are coupled. Conventionally, however, the heat transfer characteristics of fins are determined from the given literature value of the heat transfer coefficient that is assumed constant over the entire fin surface. In this conventional approach, henceforth called the simple model, the actual fin–fluid interaction is not taken care of. The heat transfer coefficient actually varies along the fin surface, and depends upon the fin conductance as well as the Reynolds and Prandtl numbers. The correct method, henceforth called the complete model, is to solve the conduction problem for the fin and the convection problem for the fluid simultaneously.

For rectangular fins complete model studies have been carried out by Sparrow and Chyu [1] for forced convection, by Sparrow and Acharya [2] for natural convection, and by Sunden [3, 4] for mixed convection but only for a fixed Prandtl number of 0.7. A very simple method, based on a similar solution approach, was reported in ref. [5] for a wide range of Prandtl numbers. The effect of Prandtl number on the heat transfer from a rectangular fin has also been studied by Sunden [6]. For cylindrical fins complete model studies have been carried out in refs. [7, 8], and in ref. [9] for forced, natural and mixed convective flow, respectively, but for a Prandtl number of 0.7 only. Moreover, the analysis of Huang and Chen [7] has some deficiencies, as detailed in ref. [9].

† On sabbatical leave from Indian Institute of Technology, Kanpur, India.

The main objective of the present work is to analyze the heat transfer from cylindrical fins cooled or heated by a high or low Prandtl number fluid for various values of the conduction–convection parameter. Another objective is to compare the simple and complete models for the cylindrical fin under these conditions. While the fin conduction equation has heretofore been solved by either a relaxation procedure [3, 4] or a direct matrix inverse method [7, 8], we use the simple Runge–Kutta method of integration [5, 9]. Our method is very inexpensive compared to the relaxation method or to the matrix inverse method.

2. ANALYSIS

Consider a laminar free stream with velocity u_∞, temperature T_∞, conductivity K, kinematic viscosity ν, and thermal diffusivity α approaching a cylindrical thin fin which is aligned parallel to the oncoming flow. The fin of radius r_0, length L ($\gg r_0$) and conductivity K_f is attached to a base held at temperature T_0. The flow takes place from the tip ($x = 0$) to the base ($x = L$) of the fin. The temperature of the fin is $T_f(x)$, the temperature of the fluid within the boundary layer is $T(x, r)$, and the heat transfer coefficient is $h(x)$. We neglect the stagnation cooling of the fin tip, and consider a long fin so as not to be concerned with the separated region near the base of the fin.

Defining the dimensionless variables

$$U = u/u_\infty, \quad X = x/L, \quad V = v\,Re^{1/2}/u_\infty,$$

$$R = r\,Re^{1/2}/L, \quad R_0 = r_0\,Re^{1/2}/L, \quad \theta = (T-T_\infty)/(T_0-T_\infty),$$

$$\theta_f = (T_f-T_\infty)/(T_0-T_\infty), \quad Re = u_\infty L/\nu, \quad Pr = \nu/\alpha$$

the one-dimensional fin conduction equation [10] with negligible tip leakage is

$$\frac{d^2\theta_f}{dX^2} = N_{cc} h_N(X)\theta_f \tag{1}$$

with boundary conditions

$$\theta_f(X=1) = 1 \quad \text{and} \quad \frac{d\theta_f}{dX}(X=0) = 0. \tag{2}$$

The boundary layer equations for the laminar, uniform property, viscous flow are

$$\frac{\partial(RU)}{\partial X} + \frac{\partial(RV)}{\partial R} = 0 \tag{3}$$

$$U\frac{\partial U}{\partial X} + V\frac{\partial U}{\partial R} = \frac{1}{R}\frac{\partial}{\partial R}\left(R\frac{\partial U}{\partial R}\right) \tag{4}$$

$$U\frac{\partial \theta}{\partial X} + V\frac{\partial \theta}{\partial R} = \frac{1}{Pr}\frac{1}{R}\frac{\partial}{\partial R}\left(R\frac{\partial \theta}{\partial R}\right) \tag{5}$$

with the boundary conditions

$$U = 0 = V, \quad \theta = \theta_f(X) \quad \text{at } R = R_0$$

$$U \to 1, \quad \theta \to 0 \quad \text{as } R \to \infty$$

and

$$U = 1, \quad \theta = 0 \quad \text{at } X = 0, R > R_0$$

where the conduction–convection parameter, $N_{cc} = (2KL/K_f r_0)Re^{1/2}$, is the ratio of conductive to convective resistance; the dimensionless heat transfer coefficient $h_N(X) = (h(X)L/K)Re^{-1/2}$; and u and v are the velocity components along the axial and radial coordinates x and r, respectively.

The heat transfer coefficient $h_N(X)$ to be used in the conduction equation is an outcome of the solution of the boundary layer equations while the thermal boundary condition to the boundary layer equations is an outcome of the solution to the conduction equation. The coupling between the conduction and boundary layer equations is expressed by the requirement that the heat flux and the temperature be continuous at the fin–fluid interface. Hence the coupling is provided by

$$h(x)[T_f(x)-T_\infty] = -K\frac{\partial T}{\partial r}(r = r_0). \tag{6}$$

3. SOLUTION

The boundary layer equations (3)–(5) are solved by a finite difference marching technique, which is a modified version of the one described by Hornbeck [11] for flow in a circular pipe. Due to the non-linear nature of these equations, an iterative solution using the Thomas algorithm at each marching X-location is carried out. This iterative solution is coupled with the fin conduction equation so as to get the correct fin temperature and heat transfer coefficient as a function of length along the fin.

For the solution of the second-order linear ordinary differential equation (1), two linearly independent solutions θ_{f1} and θ_{f2} are assumed such that

$$\theta_{f1}(X=1) = 1, \quad d\theta_{f2}(X=1)/dX = 0 \tag{7}$$

and

$$\theta_{f2}(X=1) = 0, \quad d\theta_{f2}(X=1)/dX = 1. \tag{8}$$

Equation (1) is integrated twice from $X = 1$ to 0, first with initial conditions (7) and then with initial conditions (8) using the fourth-order Runge–Kutta method yielding $\theta_{f1}(X)$ and $\theta_{f2}(X)$. Then the general solution of equation (1) is a linear combination of $\theta_{f1}(X)$ and $\theta_{f2}(X)$ such that

$$\theta_f(X) = a\theta_{f1}(X) + b\theta_{f2}(X) \tag{9}$$

where the arbitrary constants a and b are determined from boundary conditions (2).

The following iterative procedure is followed for the solution of equations (1)–(6).

(1) A uniform fin temperature distribution such as $\theta_f(X) = 1$ is assumed to initialize the iteration process.

(2) Using this $\theta_f(X)$ as the boundary condition the boundary layer equations (3)–(5) are solved and the local heat transfer coefficient $h(X)$ is calculated using equation (6).

(3) With this $h(X)$, the fin conduction equation (1) is solved to get $\theta_f(X)$.

(4) Steps 2 and 3 are repeated until convergence.

4. COMPUTATIONAL DETAILS

Following a step size study, the step size in the marching direction (ΔX) was taken as 5×10^{-5} near the tip of the fin ($X = 0$) and gradually increased with X up to $X = 1/2$. Beyond $X = 1/2$, ΔX was gradually decreased up to $X = 1$ in order to take care of steeper fin temperature gradients. Along the cross-stream direction very fine grids of size $\Delta R = 0.04$ were concentrated near the fin surface and comparatively coarser grids ($\Delta R = 0.1$) were imposed in the region far away from the fin surface.

For the convergence of the solution the difference in fin temperature values between two consecutive iterations was kept such that

$$[\theta_f^{m+1}(X) - \theta_f^m(X)]/\theta_f^{m+1}(X) \leqslant \varepsilon_1, \quad \text{for } 0 \leqslant X \leqslant 1$$

where m represents the iteration index and ε_1 was taken as 10^{-6} for the results presented here. For the convergence of the boundary layer equations the difference in the velocity distributions between two consecutive iterations was kept such that

$$[U^{m+1}(R) - U^m(R)]/U^{m+1}(R) \leqslant \varepsilon_2, \quad \text{for } R_0 \leqslant R \leqslant R_\infty$$

where R_∞ is the radius of the outer edge of the axisymmetric boundary layer and ε_2 was kept at 10^{-3}. We found almost no change in results when ε_2 was taken as 10^{-6} except for the additional computer time. A maximum of eight iterations were required for the conduction equation for the largest

N_∞ value. We may also mention that no relaxation was necessary.

For checking our numerical scheme we compared our results for an isothermal fin ($N_\infty = 0$) of radius $R_0 = 4/3$ with the local non-similarity solution of Yu and Sparrow [12] for an isothermal cylinder. Excellent agreement was obtained. We also compared the overall fin heat transfer rate Q_N with the heat flux integrated over the convecting fin surface. The deviation was less than 0.6% for the entire range of parameters considered. In order to test the method by which we solve the conduction equation, we fed a uniform value of the heat transfer coefficient into it and compared its results with the analytical solution obtained from the simple model. The results matched exactly.

5. RESULTS AND DISCUSSION

Allowing the Prandtl number to vary in the range $0.01 \leqslant Pr \leqslant 100$ and the conduction–convection parameter to vary in the range $0 \leqslant N_\infty \leqslant 6$, dimensionless values of the local heat transfer coefficient h_N, average heat transfer coefficient from an isothermal fin $\bar{h}_N$, local fin temperature θ_f, local heat flux q_N, overall fin heat transfer rate Q_N, and fin effectiveness ϕ based on an isothermal fin were determined from the relations

$$h_N = (hL/K)Re^{-1/2}$$

$$\bar{h}_N = \int_0^1 h_N(X)\,\mathrm{d}X$$

$$q_N = \frac{qL}{K(T_0-T_\infty)}Re^{-1/2} = h_N\theta_f$$

$$Q_N = \frac{Q}{r_0K(T_0-T_\infty)}Re^{-1/2} = \frac{2\pi}{N_\infty}\frac{\mathrm{d}\theta_f}{\mathrm{d}X}(X=1)$$

and

$$\phi = Q_N/2\pi\bar{h}_N$$

where q and Q are the dimensional counterparts of q_N and Q_N, respectively. The conduction equation for θ_f in the simple model yields [10]

$$\theta_f = \cosh\,(N_\infty\bar{h}_N X^2)^{1/2}/\cosh\,(N_\infty\bar{h}_N)^{1/2}$$

and the relations for q_N, Q_N and ϕ in the simple model are

$$q_N = \bar{h}_N\theta_f$$

$$Q_N = 2\pi(\bar{h}_N/N_\infty)^{1/2}\tanh\,(N_\infty\bar{h}_N)^{1/2}$$

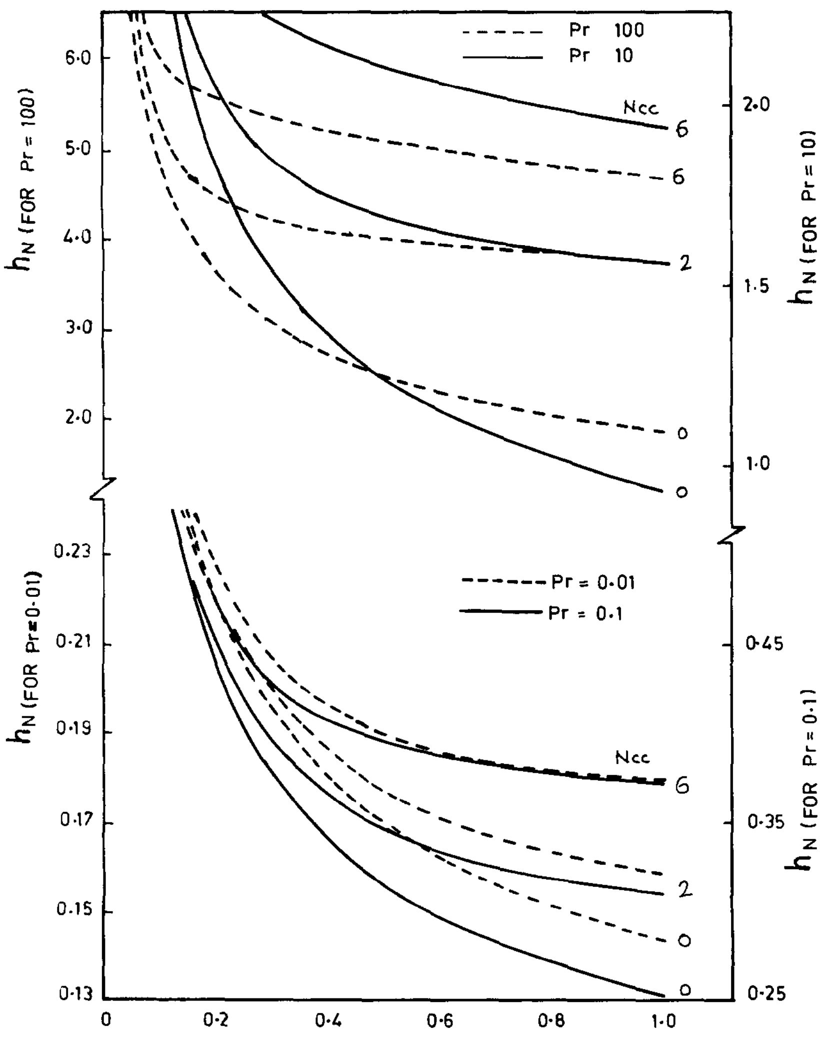

FIG. 1. Local heat transfer coefficient ($R_0 = 4$).

and

$$\phi = \tanh (N_{cc}\bar{h}_N)^{1/2}/(N_{cc}\bar{h}_N)^{1/2}.$$

The dimensionless fin radius R_0 has been kept at 4.0 for the results presented here.

Figure 1 depicts the local heat transfer coefficient as a function of X for various Pr and N_{cc} values. Note the different ordinate scales for different Prandtl numbers. Unlike the uniform value assumed in the simple model, the heat transfer coefficient decreases monotonically from the tip to the base of the fin for all N_{cc} and Pr values as the boundary layer grows along the flow direction. However, it increases with both N_{cc} and Pr, because an increasing N_{cc} means higher convective effects and/or smaller fin radius r_0, and an increasing Pr means smaller thermal boundary layer thickness. The average heat transfer coefficient $\bar{h}_N$ from an isothermal fin is presented in Table 1 for various Pr values. In the case of an isothermal cylindrical fin the average heat transfer coefficient $\bar{h}_N$ is found to be nearly proportional to $Pr^{0.3}$, rather than to Pr^n with $n \geq 1/3$ for cross flow over a cylinder. It may also be recalled from ref. [9] that $\bar{h}_N$ decreases or increases as the fin radius increases or decreases.

The local heat flux variation is presented in Fig. 2 along with the prediction of the simple model. The heat flux predicted by the simple model is very different from what really prevails. The difference between the two models is maximum at low N_{cc} and Pr values near the tip region, and it decreases as N_{cc} and Pr increase. However, for high Prandtl numbers this difference increases at the base of the fin. Despite this discrepancy in the local heat flux, the areas under the corresponding heat flux curves of the two models are almost equal for all N_{cc} and Pr values.

Table 1. Average heat transfer coefficient ($\bar{h}_N$) for an isothermal fin ($R_0 = 4$)

Pr	$\bar{h}_N$
0.01	0.2034
0.1	0.4004
0.7	0.7258
10.0	1.6257
100.0	3.1458

Figure 3 displays the fin temperature distribution from both the models for the two extreme Pr values. The fin becomes more and more nonisothermal as either N_{cc} or Pr increases due to low fin conductance and high convective effects. The simple model overpredicts the temperature over the entire fin length except at the base, and the percentage error in its prediction increases with both N_{cc} and Prandtl number.

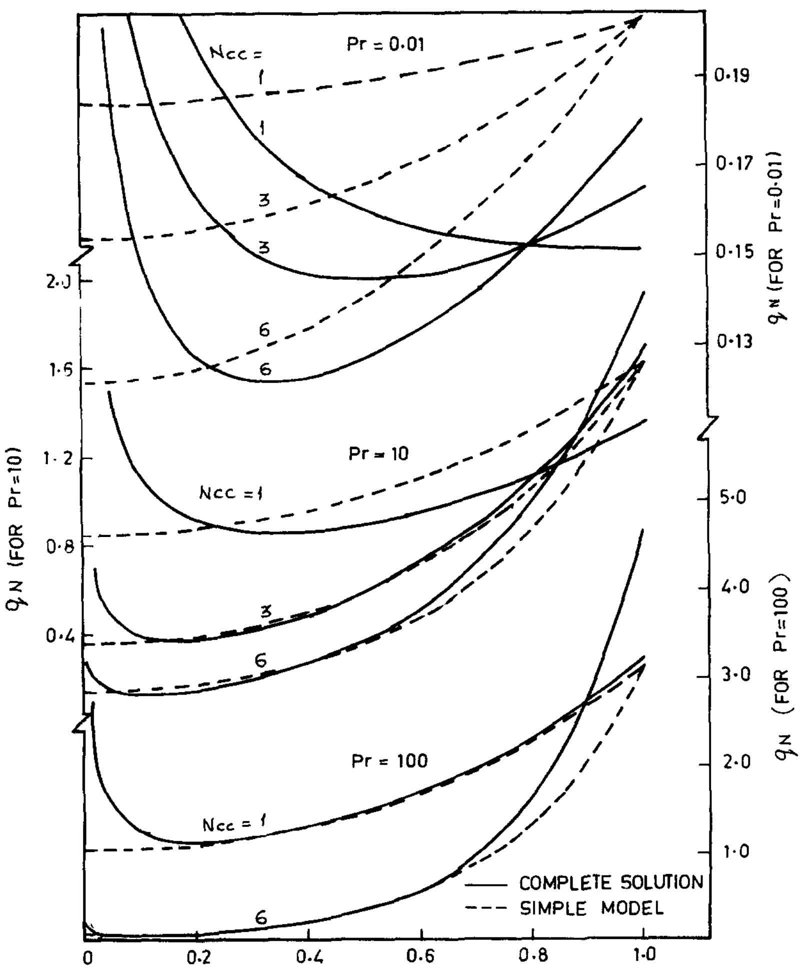

FIG. 2. Local heat flux along the fin surface ($R_0 = 4$).

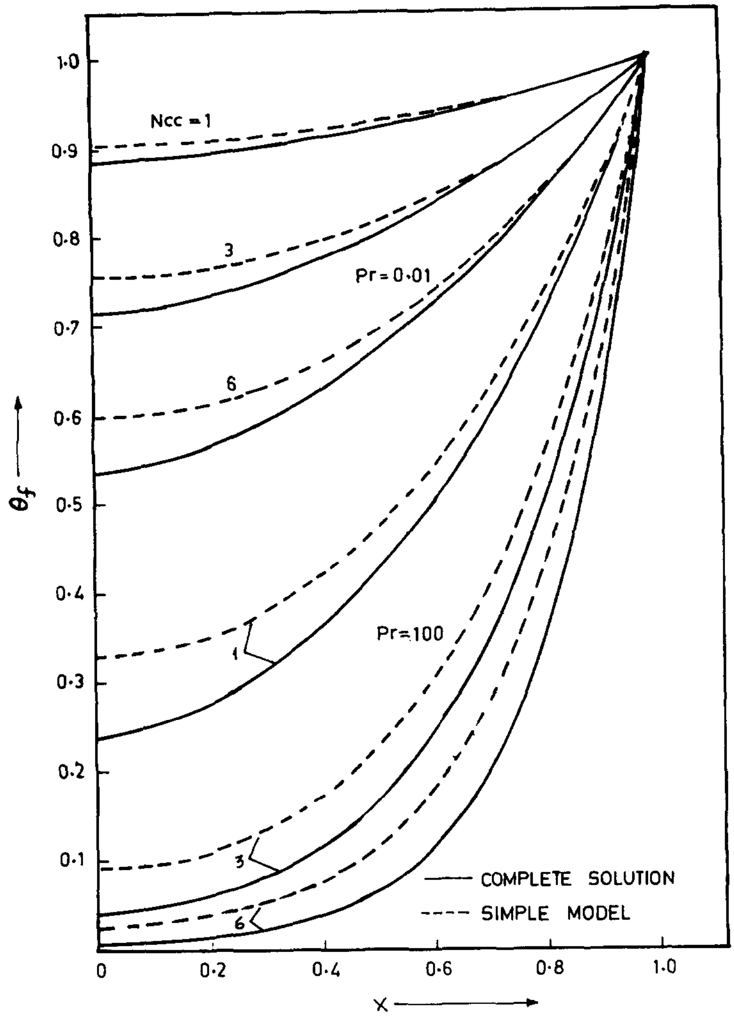

FIG. 3. Local fin temperature distribution ($R_0 = 4$).

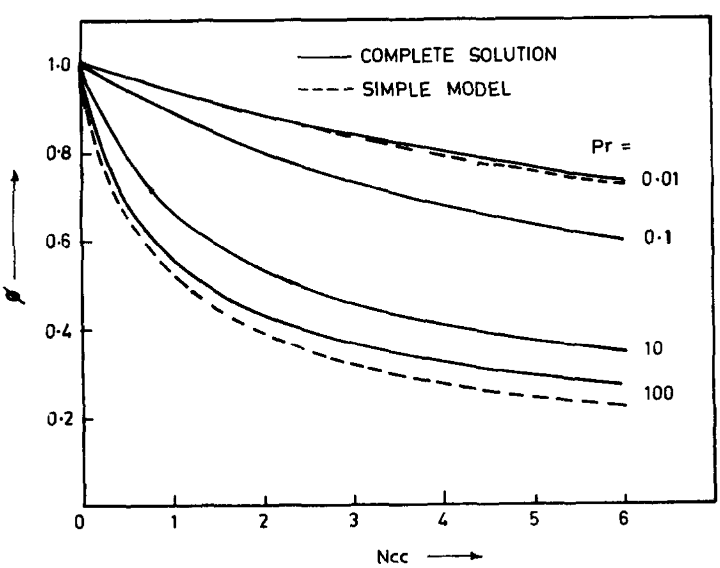

FIG. 4. Fin effectiveness based on an isothermal fin ($R_0 = 4$).

Figure 4 depicts the fin effectiveness ϕ based on an isothermal fin for both the complete and simple models. The effectiveness ϕ decreases as N_{∞} and Pr increase since the fin becomes more and more nonisothermal due to decreased fin conductance ($K_f r_0$) and/or increased convective effects. Though the difference in ϕ for the two models is small, it may be pointed out that the higher the values of N_{∞} and Pr the more conservative the simple model gets. These results are for $R_0 = 4$. We know [9] that the fin temperature becomes less uniform as R_0 decreases due to lower fin conductance. Thus, the fin effectiveness will decrease with decreasing R_0. The overall heat transfer rate Q_N from the fin can be easily calculated from Fig. 4 and Table 1, and is therefore not presented separately.

6. CONCLUSIONS

A numerical solution of the coupled fin conduction equation and the laminar, forced convective boundary layer equations for a cylindrical fin has been carried out. The effects of Prandtl number and the conduction–convection parameter on the heat transfer characteristics have been studied. It has been found that the dimensionless average heat transfer coefficient for an isothermal cylindrical fin is nearly proportional to $Pr^{0.3}$. While the simple model predicts the fin effectiveness and the overall heat transfer rate from the fin within tolerable accuracy over the entire range of Pr values, its predictions of local heat flux and fin temperature are in substantial error.

Acknowledgements—The computing facility availed at the Indira Gandhi Centre for Atomic Research, Kalpakkam, India, is gratefully acknowledged. The first author would also like to acknowledge the support from The Ohio State University during his sabbatical.

REFERENCES

1. E. M. Sparrow and M. K. Chyu, Conjugate forced convection–conduction analysis of heat transfer in a plate fin, *ASME J. Heat Transfer* **104,** 204–206 (1982).
2. E. M. Sparrow and S. Acharya, A natural convection fin with a solution-determined nonmonotonically varying heat transfer coefficient, *ASME J. Heat Transfer* **103,** 218–225 (1981).
3. B. Sunden, Conjugate mixed convection heat transfer from a vertical rectangular fin, *Int. Commun. Heat Mass Transfer* **10,** 267–276 (1983).
4. B. Sunden, A numerical investigation of coupled conduction–mixed convection for rectangular fins, *Proc. 3rd Int. Conf. Numer. Meth. in Laminar and Turbulent Flow*, Aug. 1983, Seattle, pp. 809–819. Pineridge Press, Swansea (1983).
5. V. K. Garg and K. Velusamy, Heat transfer characteristics for a plate fin, *ASME J. Heat Transfer* **108,** 224–226 (1986).
6. B. Sunden, The effect of Prandtl number on conjugate heat transfer from rectangular fins, *Int. Commun. Heat Mass Transfer* **12,** 225–232 (1985).
7. M. J. Huang and C. K. Chen, Vertical circular pin with conjugated forced convection–conduction flow, *ASME J. Heat Transfer* **106,** 658–661 (1984).
8. M. J. Huang, C. K. Chen and J. W. Cleaver, Vertical circular pin with conjugated natural convection–conduction flow, *ASME J. Heat Transfer* **107,** 242–245 (1985).
9. K. Velusamy and V. K. Garg, Heat transfer from a cylindrical fin in combined free–forced flow, *Int. J. Heat Fluid Flow* 9(2), 233–240 (1988).
10. E. R. G. Eckert and R. M. Drake, *Analysis of Heat and Mass Transfer.* McGraw-Hill, Tokyo (1972).
11. R. W. Hornbeck, Numerical marching techniques for fluid flows with heat transfer, NASA SP-297, Washington, DC (1973).
12. H. S. Yu and E. M. Sparrow, Local nonsimilarity thermal boundary layer solutions, *ASME J. Heat Transfer* **93,** 328–334 (1971).

Int. J. Heat Mass Transfer. Vol. 32, No. 1, pp. 192–195, 1989
Printed in Great Britain
0017-9310/89 $3.00+0.00

Transient forced convection heat transfer from a circular cylinder in a saturated porous medium

SHIGEO KIMURA
Government Industrial Research Institute, Tohohu, 4-2-1 Nigatake, Sendai 983, Japan

(*Received* 22 *March* 1988 *and in final form* 23 *June* 1988)

1. INTRODUCTION

TRANSIENT heat transfer from a cylinder placed in a fluid-saturated porous medium is considered. It is assumed that the flows are perpendicular to the cylinder axis and the velocities are sufficiently large to neglect the buoyant force caused by temperature differences, but small enough to ensure the validity of Darcy's law. When the wall temperature of the cylinder is raised to T_w and maintained at that temperature thereafter, the thin thermal boundary layer is formed during a small time period. The thermal layer then grows with time until the radial thermal diffusion is eventually balanced with the cross convection. The associated steady-state problem was first considered by Cheng [1] with boundary layer approximations. The analysis has been recently extended by Kimura [2] to cylinders of elliptic cross sections with integral methods. The forced convection from a cylinder has important applications in an area for shallow geothermal energy use and development. For instance a shallow aquifer, which is kept at a temperature of about 10°C during the winter time, is a possible heat source for house heating and other uses in cold regions. Development of heat extraction techniques from shallow aquifers with cylindrical heat exchangers, i.e. large heat pipes, requires knowledge on heat transfer described in the present problem.

2. MATHEMATICAL FORMULATION AND SOLUTION PROCEDURE

Nondimensionalized conservation equations for momentum and energy with the assumption of Darcy's law and